

Point Defect Studies in Gold by Electron Irradiation at Low Temperatures. III. Resistivity Recovery from 240–340°K (Stage III)*

WALTER BAUER AND A. SOSIN

Atoms International, Division of North American Aviation, Inc., Canoga Park, California

(Received 25 May 1964)

We have studied the recovery of electrical resistivity of 99.999%-pure gold after 2-MeV electron irradiation near 80°K. It was found that the recovery in the last 55% of stage III (240–340°K) is characterized by second-order annealing kinetics with an activation energy of 0.80 ± 0.04 eV. The second-order nature of the recovery and other related evidence indicate that the recovery process consists of the random recombination of interstitials and vacancies.

I. INTRODUCTION

IN two previous papers^{1,2} hereby referred to as I and II, we presented experimental evidence and related theoretical arguments that permanent displacements of gold atoms occur mainly in the $\langle 100 \rangle$ direction after irradiation by electrons with energy of 2 MeV or less and that practically no long-range migration or random recombination of point defects takes place between 15 and 240°K.

In this paper we present experimental results and analysis related to the recovery of electrical resistivity in stage III (240–340°K). Since only Frenkel pairs of varying separation are produced with 2-MeV electron bombardment, and since the irradiations are carried out at a temperature at which there is no appreciable, if any, defect mobility, the interpretation of the results is not complicated by the production of significant concentrations of divacancies or di-interstitials during the irradiation. By way of comparison, the interpretation of recovery after heavy-particle irradiation or plastic deformation is inherently encumbered by such complications. The study of the stage III resistivity recovery in gold after electron irradiation is particularly important since it accounts for approximately 50% of the total recovery and the recovery at 340°K is almost complete.

The activation energy characterizing the recovery in stage III has been previously reported to be 0.72 ± 0.04

eV after electron irradiation,³ 0.80 ± 0.04 eV after 10-MeV proton irradiation,⁴ 0.71 ± 0.02 eV after plastic deformation,⁵ and 0.75 ± 0.06 eV after 200 eV argon-ion bombardment.⁶ It is important to point out that the energy of motion of a single vacancy is known⁷ to be 0.82 ± 0.05 eV.

The experimental methods utilized in the present work are described in Sec. II. Section III deals with the experimental results. In Sec. IV we present a discussion of the stage III recovery mechanisms. Finally, a model for the production and recovery of point defects in gold by 2 MeV electron irradiation is presented in Sec. V.

II. EXPERIMENTAL METHODS

The (99.999%-pure) gold specimens used were in the form of 0.004-in.-diam wire purchased from Sigmund Cohn Corporation. The specimen preparation has been discussed in I. The residual resistivity of the specimens used in these experiments ranged from 2.51×10^{-9} Ω -cm to 2.68×10^{-9} Ω -cm. The residual resistivity and resistivity increase were calculated in the same manner as described in I. With a measuring current of 1 A, the experimental uncertainty of the resistivity measurements was $\pm 10^{-12}$ Ω -cm.

All irradiations were conducted near 80°K. The basic method and equipment employed is very similar to that used by Sosin and Rachal.⁸ The specimen configuration

TABLE I. Annealing and measurement liquids.

| Coolant | Temperature | Temperature variation | Purpose |
|-----------------|-------------|--------------------------|-------------------------|
| Liquid helium | 4.2°K | | Measurement |
| Liquid nitrogen | 78°K | | Storage and irradiation |
| Petroleum ether | 230–290°K | $\pm 0.05^\circ\text{K}$ | Anneal |
| Water | 300–350°K | $\pm 0.01^\circ\text{K}$ | Anneal |

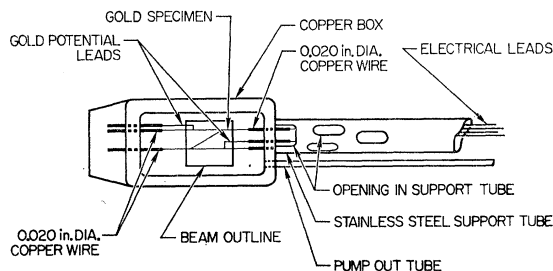


FIG. 1. Specimen holder used for irradiations near 80°K and for direct immersion into annealing liquids (ether and water) and liquid-helium storage vessels.

* This work was supported by the U. S. Atomic Energy Commission.

¹ W. Bauer and A. Sosin, Phys. Rev. **135**, A521 (1964).

² W. Bauer and A. Sosin, Phys. Rev. **136**, A255 (1964).

³ J. W. Kauffman and R. W. Wullaert, Conference on the Recovery of Metals, Delft, 1962 (unpublished).

⁴ F. Dworschak, K. Herschbach, and J. S. Koehler, Phys. Rev. **133**, A 293 (1964).

⁵ W. Schuele, A. Seeger, D. Schumacher, and K. King, Phys. Stat. Solidi **2**, 1199 (1962).

⁶ J. A. Venables and R. W. Balluffi, Bull. Am. Phys. Soc. **9**, 295 (1964).

⁷ J. E. Bauerle and J. S. Koehler, Phys. Rev. **107**, 1493 (1957).

⁸ A. Sosin and L. H. Rachal, Phys. Rev. **130**, 2238 (1963).

TABLE II. Recovery in stage III of gold.

| Author | Source of defects | Method of analysis | Activation energy (eV) | Kinetics | Temperature range |
|--------------------------------------|---------------------------------------|---------------------------------------|------------------------|----------|-------------------|
| Dworschak <i>et al.</i> ^a | 10-MeV protons | Primak | 0.80±0.04 | 2 | 240–290°K |
| Kauffman and Wullaert ^b | 2–3-MeV electrons | Slope change | 0.72±0.04 | | 270–350°K |
| Present work | 2-MeV electrons | Meechan and Brinkman | 0.80±0.04 | 2 | 290–330°K |
| Schuele <i>et al.</i> ^c | Cold work | Meechan and Brinkman | 0.71±0.02 | 2 | 230–290°K |
| Venables and Balluffi ^d | Ion bombardment (electron microscope) | Calculated from diffusion coefficient | 0.75±0.06 | | at 300°K |

^a See Ref. 4.^b See Ref. 3.^c See Ref. 5.^d See Ref. 6.

and irradiation box are shown in Fig. 1. The specimen was soldered to 0.020-in.-diam copper wires, each of which led out of a box through a glass-to-metal seal. At the tube end of the box, holes were purposely drilled into the support tube so as to allow immersion of the lead-in wires directly into the cryogenic or annealing liquids. A 0.0005-in.-thick copper foil was soldered to the top of the box to avoid specimen contact with the liquids. The pumpout tube was used to evacuate the box or to fill it with helium gas. Within the precision of measurement, the temperature of the specimen, during annealing pulses, was the same as that of the liquid with or without helium gas in the box during measurement and annealing. The purpose of the helium gas in the specimen box was to reduce the specimen temperature during irradiation. Table I lists the various liquids used during the anneal and their temperature variation.

To eliminate the need of a correction for the time required for the specimen to reach the temperature of the annealing bath after immersion, the following procedure was used. The sample holder was immersed in an intermediate bath held at 10°K below the temperature of the annealing bath for 45 sec. This was sufficient time for the specimen to reach the intermediate bath temperature. Since the previous anneal was performed at this temperature for at least 1800 sec, no significant time correction is necessary for this step. After immersion into the annealing bath the specimen reached a temperature within 1° of the bath in a few seconds, and the bath temperature in approximately 10 sec. The corrections for these times are less than the corresponding experimental error in the resistance readings. The temperatures of the baths were measured by a copper-constantan thermocouple and regulated by balancing the heat supplied by a hot source (a knife-edge heater) against a cold sink (a copper rod, one end of which is immersed in the annealing bath, the other in liquid nitrogen or ice).

III. EXPERIMENTAL RESULTS

Three methods are commonly used to analyze the recovery of resistivity. These methods are listed in Table II and described in more detail in the appropriate references. Only the slope-change method and the

Meechan and Brinkman (MB) method,⁹ ordinarily used to determine activation energies, do not involve a choice of a frequency factor. Furthermore, the Primak analysis requires some assumptions concerning the kinetics of the annealing processes (although the results may not depend strongly on the kinetics). We have chosen to use principally the MB method, but we have also attempted to use the slope-change technique by measuring the recovery in 1-h sequential isothermal anneals in 10° steps. The experimental scatter in the values of the activation energy determined by the slope-change method was too large to make the average value meaningful. This difficulty is due to the fact that the value of the activation energy depends directly on the logarithm of the initial slope of the recovery as a function of time. The determination of the slope involves an extrapolation of the data to very short annealing times, which is subject to a relatively large error.

For the MB analysis, an isochronal anneal and one long isothermal anneal with comparable concentration of defects and identical specimens are required. The experimental results are summarized in Table III. The isochronal and isothermal recovery of run I is shown in Figs. 2 and 3, respectively, and the isochronal and isothermal recovery of run II is shown in Figs. 4 and 5, respectively. All irradiations were performed near 80°K using the apparatus and methods described in Sec. II.

A. Activation Energy

In the MB analysis, the recovery of a pair of specimens with closely identical histories (usually the same specimen damaged to the same dose in two consecutive

TABLE III. Experimental results of liquid-nitrogen irradiations.

| Run | Anneal | Residual resistivity (Ω-cm) | Damage remaining after pulse at 233°K (Damage in stage III) (Ω-cm) |
|-----|------------|-----------------------------|--|
| I | Isochronal | 2.51×10 ⁻⁹ | 0.68×10 ⁻⁹ |
| | Isothermal | 2.57×10 ⁻⁹ | 0.64×10 ⁻⁹ |
| II | Isochronal | 2.68×10 ⁻⁹ | 2.21×10 ⁻⁹ |
| | Isothermal | 2.55×10 ⁻⁹ | 2.16×10 ⁻⁹ |

⁹ C. J. Meechan and J. A. Brinkman, Phys. Rev. **103**, 1193 (1956).

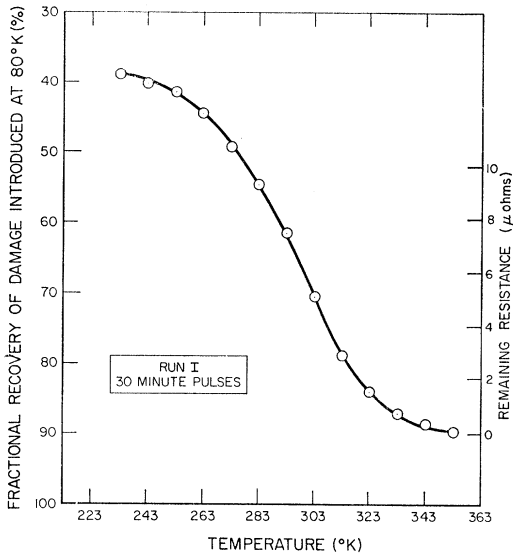


FIG. 2. Fractional resistivity recovery as a function of annealing temperature after electron irradiation at 80°K.

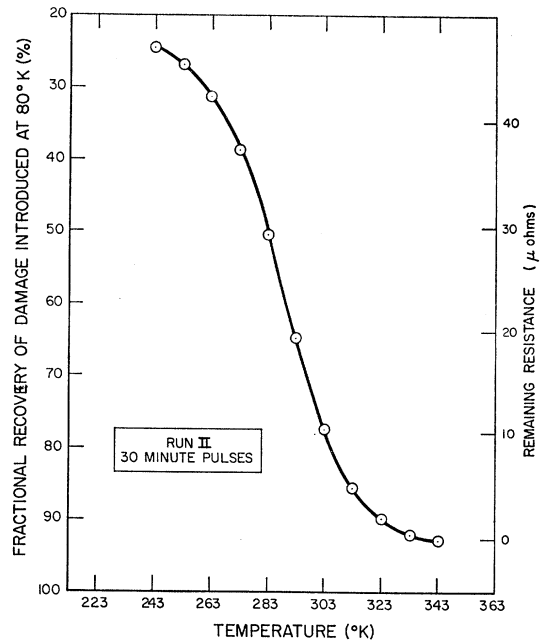


FIG. 4. Fractional resistivity recovery as a function of annealing temperature after electron irradiation at 80°K.

runs) is followed. One specimen is annealed for equal times at successively higher temperatures (isochronal); the other, at a fixed temperature for a long time (isothermal). We present a brief sketch of the analysis which is given in detail in Ref. 9.

The recovery of resistivity $\Delta\rho$ after irradiation is assumed to obey the rate equation

$$d(\Delta\rho)/dt = -F(\Delta\rho)K \exp(-E/kT), \quad (1)$$

where t represents the time, K is a constant frequency factor, k is the Boltzmann constant, T is the absolute

temperature, and E is the activation energy governing the recovery process. We define a "temperature-compensated" time parameter,

$$\theta \equiv \int_0^t \exp(-E/kT) dt = \int_{\Delta\rho_0}^{\Delta\rho} \frac{d(\Delta\rho)}{KF(\Delta\rho)}. \quad (2)$$

If the process is characterized by a single activation energy, we can write for the i th pulse, at temperature

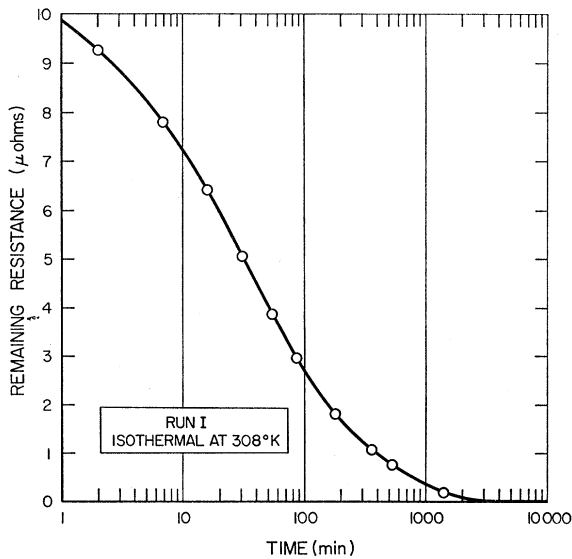


FIG. 3. Resistance remaining in the stage III recovery as a function of time at the annealing temperature of 308°K after electron irradiation at 80°K.

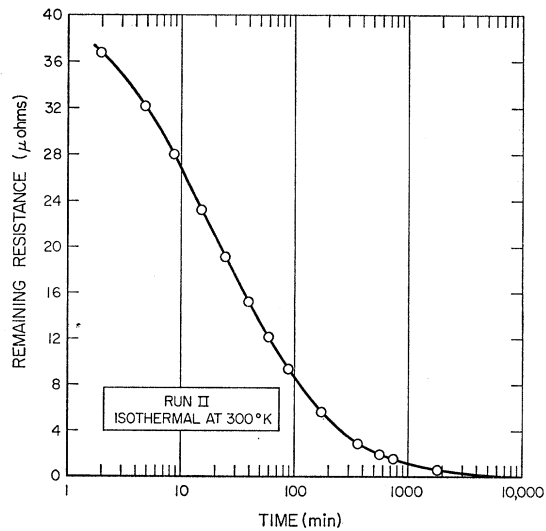


FIG. 5. Resistance remaining in the stage III recovery as a function of time at the annealing temperature of 300°K after electron irradiation at 80°K.

T_i , of the isochronally annealed specimen,

$$\ln \Delta \theta_i = \ln \Delta t - E/kT_i, \quad (3)$$

where $\Delta \theta_i$ is the change in θ during the pulse of duration Δt .

For the isothermal anneal at temperature T_a we define an annealing time, $\tau = \theta \exp(E/kT_a)$; integrating this expression we have,

$$\ln \Delta \theta_i = \ln \Delta \tau_i - E/kT_a. \quad (4)$$

In Eq. (4) $\Delta \tau_i$ is the time interval required during the isothermal anneal for the identical resistivity increment recovered during the i th pulse of the isochronal anneal. Thus the right-hand side of Eq. (2) is equal for the appropriate $\Delta \theta_i$'s and, therefore, the right-hand sides of Eqs. (3) and (4) can be set equal,

$$\ln \Delta \tau_i = C - E/kT_i, \quad (5)$$

where $C = E/kT_a + \ln \Delta t$, a constant.

A plot of $\ln \Delta \tau_i$ versus $1/T_i$ should yield a straight line with a slope of E/k for every segment of the recovery characterized by a unique activation energy. The experimental results for runs I and II are shown in Figs. 6 and 7, respectively.

The slopes of the straight lines in these figures, but

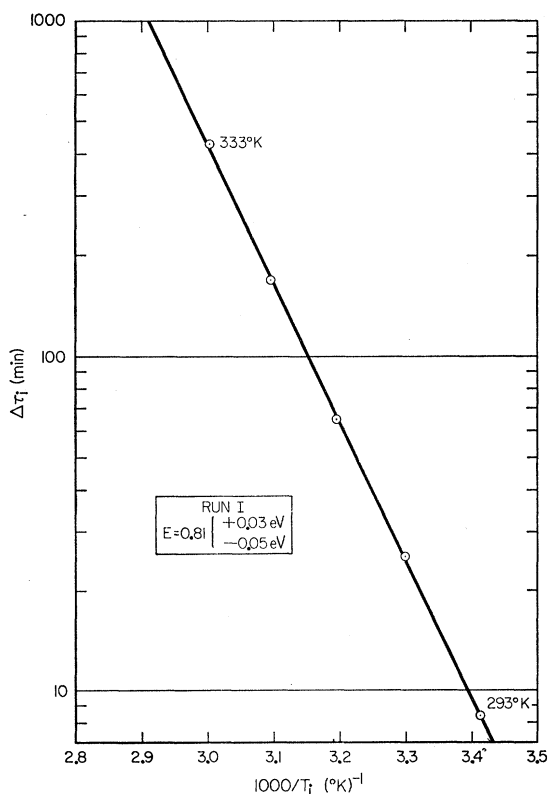


FIG. 6. A plot of Eq. (5) of the text. $\Delta \tau_i$ is the equivalent time at 308°K (data of Fig. 3) and T_i is the temperature of the i 'th isochronal pulse (data of Fig. 2). The slope of the straight line is the value of the activation energy.

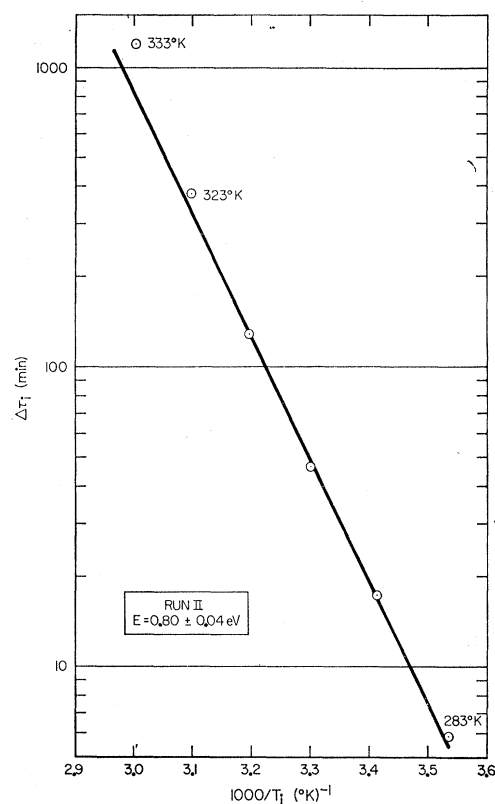


FIG. 7. A plot of Eq. (5) of the text. $\Delta \tau_i$ is the equivalent time at 300°K (data of Fig. 5) and T_i is the temperature of the i 'th isochronal pulse (data of Fig. 4). The slope of the straight line is the value of the activation energy.

not their "linearity," are sensitive to the asymptotic value to which the property recovers during the isothermal anneal. The major part of the experimental error in the determination of E is due to the uncertainty in the asymptote, rather than scatter in the experimental points. This means that there is little doubt that a uniquely activated process occurs in this temperature range, 293–333°K for run I, and 283–323°K for run II. The value of E is in excellent agreement with the findings of Dworschak *et al.*⁴ ($E = 0.80 \pm 0.04$ eV).

B. Recovery Kinetics

In Figs. 2 and 4 we note that the temperature T_e of the inflection point (point of maximum recovery rate) of the isochronal resistivity recovery of run II, is shifted to a lower temperature with respect to run I. In II we developed an expression relating a shift in the value of T_e as a function of the initial concentration of damage, assuming *second-order* recovery kinetics. Using this expression, the resistivity values of Table III, and a value of $E = 0.80$ eV, we calculate a temperature shift of 11°. This is in good agreement with the observed temperature shift of $13 \pm 2^\circ$ K. Since electron irradiation produces equal concentrations of vacancies and interstitials, the recovery below stage III is apparently

predominantly that of close interstitial-vacancy pairs (see II), and the temperature shift of stage III is as predicted, we expect the recovery in stage III to be characterized by second-order kinetics.

A direct demonstration of second-order kinetics can be achieved by use of the isothermal annealing data. If in Eq. (1) we let $F(\Delta\rho) = (\Delta\rho)^2$ for second-order kinetics, we have

$$d(\Delta\rho)/dt = -(\Delta\rho)^2 K', \quad (6)$$

where $K' = K \exp(-E/kT_a)$, a constant. Integrating Eq. (6) we have

$$1/\Delta\rho - 1/\Delta\rho_0 = K't, \quad (7)$$

where $\Delta\rho = \rho - \rho_\infty$ and $\Delta\rho_0 = \rho_0 - \rho_\infty$, where ρ_∞ is the asymptotic value of the resistivity approached during the isothermal anneal.

Thus, a plot of $1/\Delta\rho$ versus t should yield a straight line during the part of the anneal where second-order kinetics are obeyed. The experimental results are shown in Figs. 8-10. We note that the recovery follows second order kinetics in run I from 303-333°K, equivalent isochronal temperatures, and in run II from 293-333°K, equivalent isochronal temperatures.

IV. DISCUSSION OF PRESENT RESULTS

The primary observation to be drawn from the experimental results presented in this paper is that the last half of the resistivity recovery in the stage III temperature range obeys second-order kinetics with an activation energy of 0.80 ± 0.04 eV. In this section we

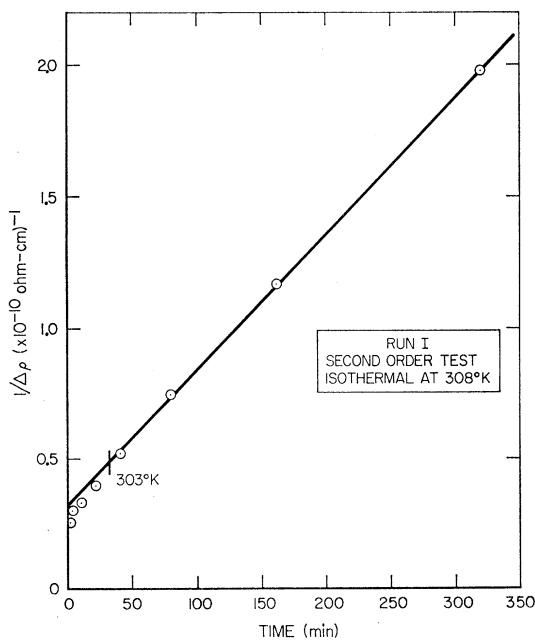


Fig. 8. A plot of the reciprocal of the resistivity remaining in stage III as a function of the annealing time at 308°K. The recovery proceeds with second-order annealing kinetics if the experimental points fall on a straight line.

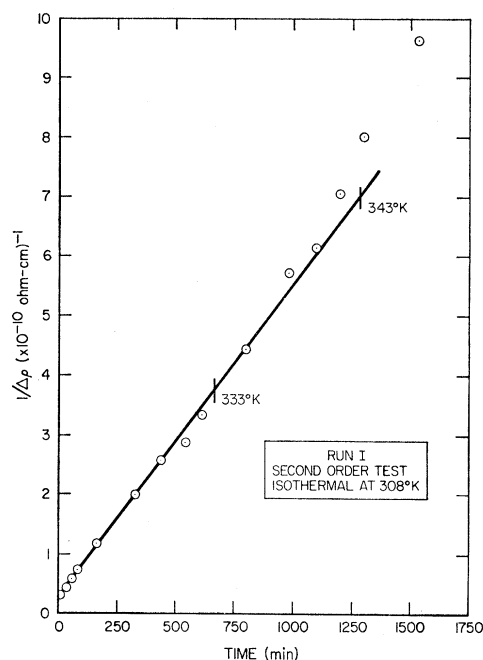


Fig. 9. A plot of the reciprocal of the resistivity remaining in stage III as a function of the annealing time at 308°K. The recovery proceeds with second-order annealing kinetics if the experimental points fall on a straight line.

discuss this result in more detail using related available data.

The observation of second-order kinetics indicates that the number of migrating defects is closely equal to the number of sinks throughout the recovery process. Since no long-range migration of defects is observed in gold below stage III, and equal numbers of interstitials and vacancies are produced during electron irradiation, such a process is not consistent with the migration of defect clusters of order two or greater; that is, second-order kinetics result from the migration of single interstitials or vacancies. This conclusion follows also under the reasonable assumptions that the formation of a significant number of di-interstitials (dimers) can only result from the long-range migration of single interstitials and that, during such migration, appreciable interstitial-vacancy annihilation must occur; this has not been observed. Our conclusion that the stage III recovery cannot be due to the migration of di-interstitials is in agreement with the conclusions of Venables and Balluffi.⁶

Purely on the basis of our results, we cannot make a judgment as to which of the defects, the interstitial or the vacancy, is more mobile. The relevant information for a decision is listed:

(1) The activation energy of single-interstitial migration has been measured to be 0.75 ± 0.05 eV by Venables and Balluffi.⁶

(2) The published value of the single-vacancy migration energy is 0.82 ± 0.05 eV.⁷

Purely on the basis of these results, we can still not make a decisive judgment as to the relative mobility of the vacancy and interstitial in stage III. However, second-order kinetics may be obeyed whether the migrating defects, which we shall hereafter arbitrarily identify as interstitials, originate from ordinary lattice positions or special positions¹⁰ (i.e., deeper traps).

One can dismiss the proposition that the stage III recovery is primarily associated with release of interstitials from impurities simply on the basis of a comparison of our result with those of Dworschak *et al.*⁴ It is reasonable to assume that the stage III recovery in Dworschak's work is primarily due to the annihilation of untrapped interstitials at vacancies, since the ratio of radiation-produced defects migrating in stage III to residual impurities is approximately 80. The equivalent ratio in our experiments is approximately 0.25. Then the two experiments represent a range of 300 in the ratio of radiation-produced defects to residual impurities. Yet, the experimental results for the activation energy in our and Dworschak's work are in excellent agreement and the shift in the temperature of the stage III recovery can be accounted for by the second-order annealing kinetics and the differing concentrations of damage. Thus, we conclude that the stage III recovery in gold is intrinsic and due to the annihilation of interstitials primarily at vacancies.

V. A MODEL FOR DAMAGE AND RECOVERY IN GOLD

On the basis of the results presented in this paper and in I and II, we can formulate a consistent picture of the production and recovery of point defects in gold after

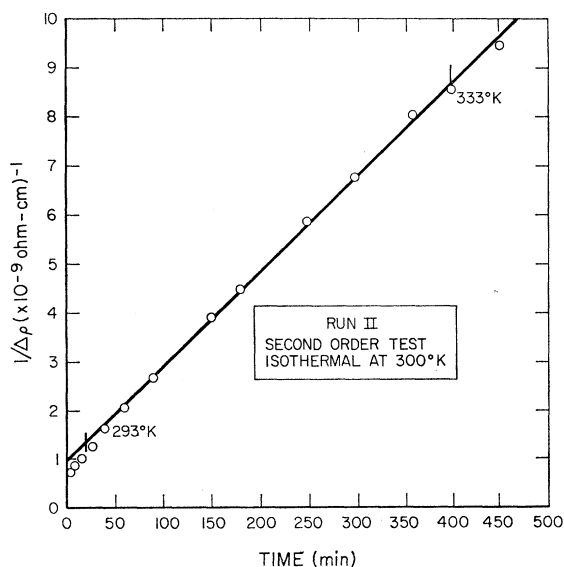


FIG. 10. A plot of the reciprocal of the resistivity remaining in stage III as a function of the annealing time at 300°K. The recovery proceeds with second-order annealing kinetics if the experimental points fall on a straight line.

¹⁰ A. C. Damask and G. J. Dienes, *Phys. Rev.* **125**, 444 (1962).

electron irradiation. During bombardment near the threshold displacement energy (and perhaps for even somewhat higher energies) there is considerable evidence that the direct displacement of gold-lattice atoms occurs only in a narrow cone about one crystallographic direction, probably the $\langle 100 \rangle$ direction (see I). Since the $\langle 100 \rangle$ direction is not favorable for long-range transport of energy and matter (energy loss per lattice distance ≈ 1.5 eV), the separation of most Frenkel pairs created in the $\langle 100 \rangle$ direction is small.

We suggest that, although no direct displacements occur in the $\langle 110 \rangle$ direction in gold in the lower energy range, considerably more long-range transport of energy may occur in the $\langle 110 \rangle$ direction (focusons) than in the $\langle 100 \rangle$ direction in gold than in copper, when the energy imparted to an atom in each is slightly above the displacement threshold. This is consistent with the results of Keefer and Sosin¹¹ who found that the saturation of dislocations by point defects during electron irradiation occurs at much lower integrated fluxes in gold than in copper, after the energy scales have been suitably adjusted. The focusons may contribute to the displacement process in two ways; first, by producing close pairs at their intersections with dislocations or stacking faults, and second, by being defocused near impurities with the subsequent production of a Frenkel pair or vacancy-interstitial-impurity complex.¹² We believe the first process to be of the order of a few percent for the dislocation densities in our annealed samples, whereas the second process might be of the order of 10%.

In order to estimate the importance of the second process we outline an order of magnitude calculation of the cross section σ for an energy transfer T_0 from a focuson to a gold atom near an impurity or to the substitutional impurity itself: (see Bauer and Sosin¹³ for development of the following expression and the meaning of the symbols)

$$\sigma = P B \Delta^{-1} \{ T_m \ln(T_m/T_0) - (T_m - T_0) - (\beta^2 + \pi\alpha\beta) \times [T_m - T_0 - T_0 \ln(T_m/T_0)] + 2\pi\alpha\beta [T_m + T_0 - 2(T_m T_0)^{1/2}] \}. \quad (8)$$

For 2.044-MeV electrons incident on gold, we have from Ref. 14

$$T_m = 66 \text{ eV}, \quad \pi\alpha\beta = 1.77, \\ B = 187 \text{ b}, \quad \beta^2 = 0.96.$$

We let

$$\Delta = 0.6 \text{ eV/atom distance}, \\ P = 10^{-4}, \text{ effective impurity concentration.}^{15}$$

¹¹ D. W. Keefer and A. Sosin, *Bull. Am. Phys. Soc.* **9**, 282 (1964).

¹² This possibility was suggested by J. A. Brinkman.

¹³ W. Bauer and A. Sosin, *J. Appl. Phys.* **35**, 703 (1964).

¹⁴ F. Seitz and J. S. Koehler, in *Solid State Physics*, edited by F. Seitz and D. Turnbull (Academic Press Inc., New York, 1956), Vol. II, p. 330.

¹⁵ This estimate is based on the assumption that there are approximately 10 lattice sites around each impurity which are effective in this displacement process. A concentration of 10^{-4} impurities is assumed to be present.

Then, we have

$$\sigma = 0.15 \text{ b for } T_0 = 33 \text{ eV,}$$

$$\sigma = 0.40 \text{ b for } T_0 = 24.2 \text{ eV.}$$

The relative concentration of defects produced by direct $\langle 100 \rangle$ displacements and by the above mechanism depends on a geometrical factor describing the efficacy for focussing the original energy of the electron into the $\langle 100 \rangle$ and $\langle 110 \rangle$ directions. On the basis of arguments advanced in I, we feel that this geometrical factor favors the $\langle 110 \rangle$ direction. The value for the displacement cross section of 2-MeV electrons incident on gold is approximately 30 b, calculated from the experimental results as reported in I, and a Frenkel resistivity of $2.7 \times 10^{-4} \Omega \text{ cm/unit concentration}$. Thus, it seems reasonable to suggest that about 10% of the total damage created may consist of either Frenkel pairs in close proximity to substitutional impurities or pairs of vacancies and impurities in interstitial positions. If the impurity atom is undersize relative to gold, it seems likely that the former may be unstable relative to the latter.

The recombination of these "hybrid Frenkel pairs" most likely gives rise to a more or less continuous recovery spectrum. One expects this spectrum to consist of a series of first-order annealing processes since the strain fields of the defects probably overlap, giving rise to nonrandom recovery as is discussed in II.

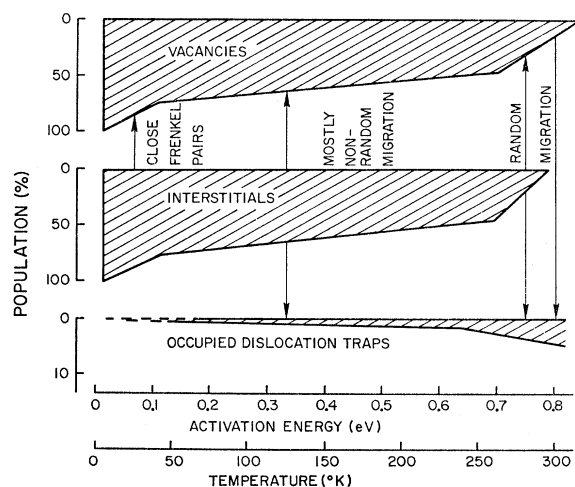


FIG. 11. A plot of the suggested annealing processes in gold after electron irradiation as a function of activation energy or annealing temperature. The induced concentration of defects by electron irradiation near 13°K is indicated as 100% population. The linear relation between activation energy and temperature is an approximation.

An interesting observation can be made in connection with the first process. When a $\langle 110 \rangle$ focuson with sufficient energy intersects a dislocation, a vacancy is probably created at the dislocation core and an interstitial is created a small distance from the dislocation. Those interstitials within the strain field of the dislocation most likely diffuse to it with a range of activation energies below the free migration energy of the interstitial. In preliminary electron irradiations of annealed and previously cold-worked samples, we have found that the recovery below 50°K in the previously cold-worked sample is slightly larger than in the annealed sample. This implies that some recovery of defects created near dislocations occurs at lower temperatures. These results in gold are different from the corresponding ones for copper. In copper it was found that the stage I recovery of the previously cold-worked sample was suppressed. Meechan *et al.*¹⁶ explained this as the conversion of crowdions to interstitials at dislocations in copper. The fact that this has not been observed in gold is additional evidence against the existence of the crowdion in gold.

To outline the model of recovery we believe to be pertinent to gold, we have plotted in Fig. 11 the population of defect configurations against the annealing temperature or appropriate activation energy of migration. Of the secondary displacement processes generated by $\langle 110 \rangle$ focusons, we indicate only the defects created at dislocations.

Our model, then, is the following. The dominant recovery mechanism up to 240°K is the nonrandom recombination of Frenkel pairs which was discussed in detail in II. Again, referring to Fig. 11, we suggest that within a narrow band of activation energies (0.65–0.80 eV) in stage III several recovery processes take place. The first portion of stage III is associated with the recombination of relatively distant Frenkel pairs and the migration of interstitials to dislocations (the latter process being only a few percent). The last half of stage III, characterized by second-order kinetics and an activation energy of $0.80 \pm 0.04 \text{ eV}$, is due to random recombination of interstitials and vacancies.

Finally, it is informative to compare our results with the results of Dworschak *et al.*⁴ Their plot of resistivity density ($\Omega\text{-cm/eV}$) as a function of activation energy in the region of stage III recovery shows a well defined peak at 0.80 eV with a "tail" extending toward lower activation energies. This is consistent with our model within which a number of processes with differing activation energies occurs, leading up to the random recombination of vacancies and interstitials at 0.80 eV.

¹⁶ C. J. Meechan, A. Sosin, and J. A. Brinkman, *Phys. Rev.* **120**, 411 (1960).